Atmos. Chem. Phys. Discuss., 13, 10661–10700, 2013
www.atmos-chem-phys-discuss.net/13/10661/2013/
doi:10.5194/acpd-13-10661-2013

Atmospheric Chemistry and Physics
Discussions
Open Access

Combined SAGE II-GOMOS ozone profile data set 1984–2011 and trend analysis of the vertical distribution of ozone

E. Kyrölä[1], M. Laine[1], V. Sofieva[1], J. Tamminen[1], S.-M. Päivärinta[1], S. Tukiainen[1], J. Zawodny[2], and L. Thomason[2]

[1]Finnish Meteorological Institute, Earth Observation Unit, P.O. Box 503, 00101 Helsinki, Finland
[2]NASA Langley Research Center, MS-475, Hampton, VA 23681-2199, USA

Received: 15 February 2013 – Accepted: 12 April 2013 – Published: 23 April 2013

Correspondence to: E. Kyrölä (erkki.kyrola@fmi.fi)

Published by Copernicus Publications on behalf of the European Geosciences Union.

Abstract

We have studied data from two satellite occultation instruments in order to generate a high vertical resolution homogeneous ozone time series of 26 yr. The Stratospheric Aerosol and Gas Experimen (SAGE) II solar occultation instrument from 1984–2005 and the Global Ozone Monitoring by Occultation of Stars instrument (GOMOS) from 2002–2012 measured ozone profiles in the stratosphere and mesosphere. Global coverage, good vertical resolution and the self calibrating measurement method make data from these instruments valuable for the detection of changes in vertical distribution of ozone over time. As both instruments share a common measurement period from 2002–2005, it is possible to intercalibrate the data sets. We investigate how well these measurements agree with each other and combine all the data to produce a new stratospheric ozone profile data set. Above 55 km SAGE II measurements show much less ozone than the GOMOS nighttime measurements as a consequence of the well-known diurnal variation of ozone in the mesosphere. Between 35–55 km SAGE II sunrise and sunset measurements differ from each other. Sunrise measurements show 2 % less ozone than GOMOS whereas sunset measurements show 4 % more ozone than GOMOS. Differences can be explained qualitatively by the diurnal variation of ozone in the stratosphere recently observed by SMILES and modelled by chemical transport models. For 25–35 km SAGE II sunrise and sunset and GOMOS agree within 1 %.

The observed ozone bias between collocated measurements of SAGE II sunrise/sunset and GOMOS night measurements is used to align the two data sets. The combined data set covers the time period 1984–2011, latitudes 60° S–60° N and the altitude range of 20–60 km. Profile data are given on a 1 km vertical grid, and with a resolution of one month in time and ten degrees in latitude. The combined ozone data set is analyzed by fitting a time series model to the data. We assume a linear trend with an inflexion point (so-called “hockey stick” form). The best estimate for the point of inflexion was found to be the year 1997 for ozone between altitudes 35 and 45 km. At all latitudes and altitudes from 25 km to 50 km we find a clear change in

ACPD
13, 10661–10700, 2013

Title Page
Abstract | Introduction
Conclusions | References
Tables | Figures
◂◂ | ▸▸
◂ | ▸
Back | Close
Full Screen / Esc
Printer-friendly Version
Interactive Discussion

ozone trend before and after the inflexion time. From 38 km to 45 km a negative trend of 0–3 % per decade at the equator has changed to a small positive trend of 0–2 % per decade except in the altitude range of 30–35 km where the ozone loss has even increased. At mid-latitudes the negative trend of 4–10 % per decade has changed to to a small positive trend of 0–2 % per decade.

1 Introduction

The stratospheric ozone decline and especially the drastic decrease of ozone over the Antarctic have been a focus of middle atmosphere research in the past 25 yr (for reviews, see Solomon, 1999; Staehelin et al., 2001). A better understanding for the reasons of ozone loss was quickly established after the ozone hole discovery and an international agreement about the control of ozone depleting substances was agreed in Montreal 1987. The restrictions have led to a decline of atmospheric chlorine, the most important substance in ozone loss, in the stratosphere since 1997. An improved understanding of the ozone loss problem along with the advances in the middle atmosphere modeling have made it possible to predict a complete recovery of stratospheric ozone between 2050 and 2070 (for a review of ozone depletion science, see WMO, 2011).

In order to follow the development of middle atmosphere ozone, global measurements are needed. Ground based instruments and sondes can monitor ozone mainly in the lower stratosphere but, in order to attain a global view of trends, satellite instruments need to be used. There are excellent long time series of the total ozone and its evolution, but in order to investigate the details of the processes involved, vertical ozone profiles are required. Several studies have used satellite measurements to study the decline of ozone and the predicted recovery (see e.g. Harris et al., 1999; Weatherhead et al., 2000; Newchurch et al., 2003; Steinbrecht et al., 2006; Randel and Wu, 2007; Steinbrecht et al., 2009; Jones et al., 2009). Weak signs of the ozone recovery have already been detected.

Past changes in ozone have taken place slowly and this pace is predicted to continue. Therefore, requirements for the stability of ozone observations are stringent. Self calibrating occultation instruments are good candidates for such a task. The SAGE II instrument (Chu et al., 1989) made 168 000 solar occultation measurements of ozone in the stratosphere and lower mesosphere from 1984 to 2005. The more recent GOMOS instrument (Bertaux et al., 2010) measured ozone in the stratosphere, mesosphere and lower thermosphere from 2002–2012 using stellar occultations. There are more than 877 000 GOMOS measurements covering both day and night. In this work we use only the GOMOS 410 000 night measurements.

In this paper we combine these two ozone data sets to create a homogeneous time series from 1984 to 2011 and look for changes in the middle atmosphere ozone profiles. We first introduce the instruments and the retrieval methods, and the applied data filtering in Sects. 2–4. The differences between the SAGE II and GOMOS ozone profiles are studied in Sect. 5 using collocated measurements in the 2002–2005 shared operation period of the two instruments. The observed bias in ozone profiles is eliminated and the two data sets are combined in Sect. 6. In Sect. 7 we introduce a time dependent model including a linear term, annual and semiannual terms as well as proxies for the solar influence and the QBO. The linear term of the model fitted is used to derive ozone trends in Sect. 8.

2 SAGE II and GOMOS measurements

SAGE II was launched in 1984 on board the ERBS satellite. The SAGE II heritage is the SAGE I solar occultation instrument (McCormick et al., 1989) that was operational in 1979–1981. Both rising and setting solar occultations were observed by SAGE II. Ozone profiles are given on a regular grid from 0.5 km to 70 km with a step of 0.5 km. In 21 yr (1984–2005) SAGE II measured 161 544 solar occultations. In Fig. 1 we show how the measurements are distributed over the years. The number of measurements is stable from 1985–1999 (with the exception of 1993) but decreases towards the end of the mission. The amount of measurements from sunrises and sunsets is nearly equal throughout the mission. In Fig. 2 we show the latitudinal distribution of measurements from SAGE II in 1985 and 2004. The latitude distribution peaks at fifty degrees and has a minimum at the equator. Sunrise and sunset measurement are similarly distributed in the beginning of the SAGE II mission but the distributions differ towards the end of the mission.

SAGE II has seven wavelength channels centered at 386, 448, 453, 525, 600, 940 and 1020 nm. The ozone, NO_2, H_2O density and the aerosol extinction profiles are retrieved from the most sensitive wavelength channels. The aerosol extinction is derived from the 1020 nm channel, O_3 from the 600 nm channel and NO_2, from the 524 nm channel.

The original SAGE II algorithm was presented in Chu et al. (1989). Subsequent improvements and validations have been discussed in several publications (e.g. Cunnold et al., 1989; Wang et al., 1992; McPeters et al., 1994; Wang et al., 1996; Steele and Turco, 1997; Cunnold et al., 2000; Wang, 2002; Burton et al., 2010). The data version used in this work is 7.0, which was issued in November 2012. The main differences with respect to the earlier version 6.2 are: (1) the ozone cross section is now the same as for GOMOS (Bogumil et al., 2003), (2) the background atmospheric data are now coming from MERRA and, (3) the vertical inversion is performed using the onion peeling technique without any smoothing. The ozone values in the new version have decreased by 1–2 % with respect to the earlier version mainly because of the change in the ozone cross section. The validation work for the new SAGE II data set is underway.

GOMOS is a stellar occultation instrument on board the ENVISAT satellite (see Bertaux et al., 2010; ESA, 2001, and https://earth.esa.int/web/guest/missions/esa-operational-eo-missions/envisat/instruments/gomos). GOMOS measures both during day and night but only nighttime measurements have been validated so far. The integration time is 0.5 s, which gives an altitude sampling resolution of 0.2–1.6 km depending on the tangent altitude and the azimuth angle of the measurement. The total number of measurements is 275 188. In Fig. 1 we show how the measurements are

ACPD
13, 10661–10700, 2013

distributed over the years and in Fig. 2 we show the latitudinal distribution of measurements in 2004 and 2010. The number of measurements peaked in 2004 and declined thereafter. An instrument problem strongly decreased the number of measurements in 2005. The latitudinal distribution is more even than for SAGE II.

The spectral ranges of GOMOS detectors are 248–690 nm, 755–774 nm, and 926–954 nm making it possible to retrieve vertical profiles of O_3, NO_2, NO_3, H_2O, O_2, and aerosols. In this work we concentrate on ozone that is retrieved from the UV-visible spectral range 248–690 nm together with NO_2, NO_3 and aerosols. The retrieved ozone profiles have a 2 km vertical resolution below 30 km and a 3 km resolution above 40 km whereas NO_2 and NO_3 have a 3 km vertical resolution at all altitudes. Details of the GOMOS retrieval algorithms and data quality are discussed in Kyrölä et al. (2010b) and Tamminen et al. (2010).

The geophysical validation of measurements with different illumination conditions is presented in Meijer et al. (2004) and more recently in van Gijsel et al. (2010). Results show that in the dark limb GOMOS ozone profile data agree within a few percent in 20–40 km with the correlative data at all latitudes excluding the polar areas.

In this work we use GOMOS data version IPF 6 issued in November 2012. The main differences with respect to the IPF version 5 are the use of a full covariance matrix in the spectral inversion that has made the error estimates of ozone more realistic, and the more accurate dark current removal that has improved the stability of the data products. The validation for the new version is underway.

3 Retrievals compared

The measurements and retrievals of these two instruments are similar but not identical (see Table 1). The Sun is an extended source of radiation whereas stars appear as point sources to satellite instruments. Rays from both radiation sources are bent by refraction where chromatic dispersion must also be taken into account. The radiation field from stars enters the atmosphere as a parallel ray bundle and is sensitive to local

ACPD
13, 10661–10700, 2013

fluctuations and to the overall altitude dependence of the neutral density. The parallelism of rays is distorted causing dilution of the radiation intensity and individual rays are affected by fluctuations leading to scintillations. These two effects are not seen in solar occultation measurements. The dilution effect can be eliminated using ray optics modeling and an a priori model for the neutral density (in the case of GOMOS ECMWF data). The scintillation effect can be eliminated to a large extent by using GOMOS fast photometers (see Sofieva et al., 2010).

GOMOS measures at 1416 wavelengths in the UV-Visible and SAGE II at seven wavelengths from the visible to the near infrared. The same constituents can be retrieved from these measurements. In both retrievals the Rayleigh extinction is first eliminated using either ECMWF operational data (altitudes lower than 1 hPa) and MSIS90 climatology (higher than 1 hPa) in the case of GOMOS and MERRA in the case of SAGE II. At the comparison altitudes these two neutral density data sets differ by 2–3 % at most. The other constituents are retrieved simultaneously in GOMOS and sequentially in SAGE II. In GOMOS the aerosols are fitted using a second order polynomial in wavelength whereas SAGE II makes use of the Mie scattering theory. The SAGE II data version 7 uses the same ozone cross section (Bogumil et al., 2003) as GOMOS. In the vertical inversion GOMOS uses the onion peeling inversion along with the target resolution Tikhonov smoothing (Sofieva et al., 2004). SAGE II uses the normal onion peeling technique without any smoothing.

The stability of the SAGE II and GOMOS instruments is the crucial underlying assumption when combining these data sets and using the combined data for ozone trend studies. The self-calibrating measurement principle diminishes possible reasons for drifts of data products. But there are factors that are immune to the firewall of self-calibration. For example, the retrievals of ozone include a priori data of atmospheric temperature and density whose accuracy may change in time. The estimation of the possible drifts in ozone measurements have been investigated using stable ground based instruments. These studies indicate at most 0.3 % yr^{-1} drift for SAGE II (see Nair et al., 2011, 2012). For GOMOS Nair et al. (2011) shows somewhat larger values.

But due to the short measurement series no conclusion can be made at this time. Furthermore, these studies have used the previous data versions of SAGE II and GOMOS. The data versions used in this work are currently being validated and studied for possible drifts.

4 Data screening

Both data sets are screened for obviously erroneous ozone profiles. For SAGE II data are screened using the error estimates as explained in the SAGE II version 7 readme-file (https://eosweb.larc.nasa.gov/project/sage2/sage2_release_v7_notes). Any profile with an error estimate larger than 10 % between 30–50 km is rejected. Data at altitudes where the error estimates are larger than 300 % or larger than 200 % below 35 km are eliminated. Data are also eliminated below the level where the aerosol extinction is greater than 0.006 km^{-1} or where the 525 nm aerosol extinction is larger than 0.001 km^{-1} and the aerosol extinction ratio 525 nm/1020 nm is smaller than 1.4. The amount of data eliminated is 5 % of all SAGE II measurements between altitudes 20–60 km. The final number of measurements used in this study is 161 000 (60° S–60° N) including profiles with flagged data points.

For GOMOS we first eliminate measurements involving stars included in the GOMOS “cool and weak stars” list (see the GOMOS disclaimer, http://earth.eo.esa.int/pcs/envisat/gomos/documentation/RMF_0117_GOM_NL__2P_Disclaimers.pdf). Any individual ozone profile is rejected if more than 40 % of the points are flagged by the retrieval processor. Moreover, we reject all profiles with the absolute value of the ozone mixing ratio exceeding 100 ppm between 10 km and 110 km or the mixing ratios is outside the range −0.5 ppm and 20 ppm from 15 km to 45 km. The amount of data eliminated is 3 % of all GOMOS measurements (after the cool and weak star elimination) between 20 and 60 km. The final number of profiles used in this study is 216 554 (in 60° S–60° N).

ACPD
13, 10661–10700, 2013

5 Comparison of SAGE II and GOMOS measurements from 2002–2005

Both SAGE II and GOMOS took measurements during the period of 2002 to 2005. During this time interval SAGE II measured 12 000 solar occultations (5800 sunrises and 6200 sunsets) and GOMOS 192 000 quality controlled stellar occultations during nighttime (zenith angle larger than 105°). The large number of measurements allows for a direct comparison between SAGE II and GOMOS ozone profiles. We use the following coincidence criteria (latitude = θ, longitude = ϕ, time = t):

$$\Delta\theta < 2°,\ \Delta\phi < 10°,\ \Delta t < 12\,\mathrm{h} \tag{1}$$

The method used to characterize the difference at each altitude, z, for a given profile is

$$\Delta(z) = 100\frac{\langle f_{\mathrm{S}}^{k}(z) - f_{\mathrm{G}}^{k}(z)\rangle}{\langle f_{\mathrm{G}}^{k}(z)\rangle} \tag{2}$$

where the brackets denote median over all the collocated measurements $k = 1, \ldots K$.

In Fig. 3 we show the difference between SAGE II and GOMOS collocated ozone profiles using the coincidence criteria defined above. We show SAGE II sunset and sunrise data separately because there is a clear difference between the values of these measurements. Above 55 km the difference between day and night ozone can be seen as negative differences between SAGE II and GOMOS. For 35–55 km there is more ozone in SAGE II sunset measurements than either GOMOS nighttime or SAGE II sunrise measurements. The overall mean SAGE II difference profile is biased towards sunset measurements as the number of sunsets clearly exceeds the number of sunrises. In the 25–35 km range the differences between all the data sets are small. Below 25 km all the differences increase again and are 5 % at 20 km.

The apparent difference between SAGE II and GOMOS ozone profiles can be attributed to various reasons. The deviations can arise from differences in instrumental behavior, retrieval techniques or real atmospheric conditions during the measurements.

ACPD
13, 10661–10700, 2013
GOMOS-SAGE
E. Kyrölä et al.

There are no indications of relevant instrumental differences between SAGE II sunrise and sunset measurements even if we acknowledge the different radiation environments immediately before the actual measurements. We know, however, that the atmospheric transmission is different between nighttime, sunset, and sunrise measurements because NO_2 has a strong diurnal variation. This was seen directly when we compared GOMOS and SAGE II transmissions at collocation points. The NO_2 content interferes with the ozone retrieval but this can be shown to be only of a minor contribution to the ozone values. Therefore, it is plausible that the observed differences between the GOMOS nighttime measurements and the SAGE II sunrise/sunset measurements reflect the real diurnal differences of the atmosphere.

The plain sunrise-sunset difference is inherent in the SAGE II data and this can be visualized if we take SAGE II sunrise and sunset measurements in the tropics (10° S–10° N). Tropical ozone values are relatively stable and the sunset-sunrise populations can be compared to each other with a good justification. The differences in 5 yr periods are shown in Fig. 4. The sunset profiles exhibit up to 10 % more ozone than the sunrise profiles between 35 km and 55 km. The situation is reversed above 55 km. Below 35 km there are no large differences except that the 2001–2005 period deviates strongly from the other periods below 25 km.

The observed large diurnal differences in ozone values at altitudes below 50 km (Figs. 3–4) are in contradiction to our understanding of ozone behaviour in the stratosphere. Chemical box models predict very small variations in the stratosphere. The recent detailed measurements of the ozone diurnal cycle by the SMILES instrument (Sakazaki et al., 2012) and simulations by chemical-transport models show, however, a clear diurnal cycle of ozone in the stratosphere. SMILES results show that the magnitude between sunrise and sunset is about 4 % (0.2 ppm), which is half of the variation of 8–10 % (0.4 ppm) seen in Fig. 4. From Fig. 3 the SAGE II sunset-sunrise difference is about 6 %. It remains unknown as to why the differences inferred from SMILES are smaller than the ones observed by SAGE II and GOMOS. It must be noted that SMILES measurements cover only a limited period from October 2009 to April 2010.

ACPD
13, 10661–10700, 2013

Title Page
Abstract | Introduction
Conclusions | References
Tables | Figures
◂◂ | ▸▸
◂ | ▸
Back | Close
Full Screen / Esc
Printer-friendly Version
Interactive Discussion

6 Combined SAGE II–GOMOS data set

In order to build a common data set from these two instruments we need to find an optimal latitude–time grid for the combined data set and decide how to address the observed bias. We will also discuss what statistical estimators are appropriate for the problem. The data sets are limited to the latitude region 60° S–60° N in order to avoid seasonal gaps in the data. The extent in time covers years 1984–2011 (there are only a few GOMOS data in 2012).

6.1 Common time–latitude grid

We need to use a spatial and temporal grid where the measurements from both instruments are collected. Zonal averaging is a natural choice as the occultation instruments sample the longitudinal dimension regularly and with sufficient density. We define the filling factor for the time–latitude grid as the percentage (from all available cells) of those latitude–time cells where at least two measurement are found. A good grid filling degree is a necessary prerequisite for the grid selection and with a coarse grid this is always achieved. A desire to resolve natural variability would, on the other hand, demand more refined grids. The mean latitude–time average filling factors for several latitude–time grids are shown in Table 2. In order to get a good coverage by both instruments, a monthly grid with the five to twenty degree latitudinal bands can be selected. In the following we use 10° latitude bands.

The relatively large size of the time–latitude cells allows natural variability of the ozone field to affect the representativity of the cell estimates. In order to quantify this we define the latitudinal or temporal asymmetry of measurements in a grid cell as

$$a_S = \frac{2\langle x - x_c \rangle}{\Delta x}. \tag{3}$$

This measures the mean location of the measurements x with respect to the center of the cell centered at x_c and having width Δx. Figure 8 shows time series of asymmetries

Discussion Paper | Discussion Paper | Discussion Paper | Discussion Paper |
ACPD
13, 10661–10700, 2013
GOMOS-SAGE
E. Kyrölä et al.

and ozone densities in the latitude band 50° N–60° N. It is clear that large variability of asymmetries takes place for both instruments. In this case, there is a small SAGE II latitudinal asymmetry followed by a considerable positive asymmetry of GOMOS measurements. This may explain the change seen in the ozone densities at 40 km between SAGE II and GOMOS. In Fig. 9 we show the time averaged latitudinal and temporal asymmetries as a function of latitude. In the northernmost latitude band the mean SAGE II latitude asymmetry is −0.13 and GOMOS is considerably larger 0.27. At other latitudes the asymmetry differences between the two instruments are smaller and probably do not cause jumps in time series of ozone density. The temporal asymmetry differences are smaller and we believe that they have a smaller impact on densities.

6.2 Removal of bias

It is clear that we cannot create a homogeneous data set from SAGE II and GOMOS without a proper consideration of the bias between these two data sets that was discussed in Sect. 5. We have shown that the local time of the measurements has a strong influence on the bias. We still have to consider if the bias also depends on other parameters of the measurements like latitude, season, or year. The small number of collocations makes this study somewhat more uncertain than the plain sunset/sunrise comparisons. Figures 5 and 6 show the mean relative differences between SAGE II and GOMOS in 2002–2005 in different latitude belts. The differences from all latitudes are reasonably close to each other except in the southernmost latitude belt for sunset measurements. By comparing years and individual months the culprit for this outlier is found to be the GOMOS-SAGE II sunset comparisons in June 2003 around 48° S. The sunset/sunrise comparison for individual years is shown in Fig. 7. The bias patterns seem stable during 2002–2005.

The easiest solution for the bias problem would be to simply ignore any sunrise-sunset difference and correct the remaining bias from either GOMOS or SAGE II data. This would, however, require a near complete similarity between the sunrise and sunset

ACPD
13, 10661–10700, 2013

data sets. Because this is not the case (see Figs. 1 and 2) we continue with the separate sunrise and sunset data.

The decisive parameter that controls the relative bias between SAGE II and GOMOS is the local hour of the measurement. Therefore, we have three measurement sets: GOMOS nighttime, and sunsets and sunrise from SAGE II. We have decided to keep the GOMOS data set as the reference and to shift the two SAGE II populations in such a way that they agree with the GOMOS data set in the common data period 2002–2005. As shown above, the bias profiles vary only slightly as a function of latitude, season, or year and we ignore these variations in this work. In this work we use the average bias profiles for sunset and sunrise SAGE II measurements. Individual profiles are shifted using the appropriate bias profile. In this way the corrected SAGE II profiles agree on average with the collocated GOMOS profiles for 2002–2005. We extend the same bias correction procedure to the SAGE II measurements from 1984 to 2001 before the common measurement period. The estimated uncertainty of the bias correction (small) is added to the error budget.

6.3 The combined data set

We have to decide what statistical estimators to us to characterize data in the grid cells extending 10° in latitude and one month in time. We first construct individual instrument data series and the averages in time–latitude cells are calculated by the median of the values (for error estimates of medians, see e.g. Kyrölä et al., 2010a). A median filtering (remove measurements that deviate more than three standard deviations from the median) is applied before the average is taken. These individual instrument time series represent the combined data set for 1984–2001 and 2006–2011. For years 2002–2005 we have measurements from both instruments. For the combined data we have decided to take the weighted mean of the medians of the individual instrument data sets. The weights are the error estimates of the individual instrument medians. It is not obvious how to evaluate the error of the resulting weighted mean. If the difference between the instrument medians is larger than their error estimates predict, there is

ACPD
13, 10661–10700, 2013
GOMOS-SAGE
E. Kyrölä et al.

a good reason to believe that the two instruments have not measured a homogeneous and stationary ozone field. To allow this kind of added uncertainty we estimate the error using the dispersion correction for weighted mean error. Figure 10 shows examples of the individual time series and the combined time series.

There are alternatives to calculate representative value in any grid cell. Instead of calculating averages (single instrument) with the median, the mean or a weighted mean could be used. The median is robust to outliers but, on the other, is deceptive to a double peak or similar structure in data distributions. A priori, in the common period 2002–2005 the weighted mean from all the measurements together could be an obvious choice. However, this approach is very sensitive to the consistent calculation of errors from both instruments. In large latitude–time cells also the neutrality of the latitudinal and temporal sampling of measurements with respect to the natural variation can be an issue as discussed in Sect. 6.1. Weighting measurements may then lead to adverse effects. These issues will be discussed in detail in the continuation paper (Laine et al., 2013).

7 Time series analysis of SAGE II and GOMOS combined data set

In order to assess the temporal evolution of ozone using the combined data sets, we carry out a time series analysis using linear multi-variate regression. It is based on fitting the average profiles $\rho(z,t)$ (z = altitude, t = time) in each latitude bin with the following model:

$$\rho^{\text{fit}}(z,t) = c(z) + L(z,t) + s(z)F_{10.7}(t) + q_1(z)F_{\text{qbo}}^{10}(t) + q_2(z)F_{\text{qbo}}^{30}(t) + \sum_{n=1}^{2}\left(a_n(z)\cos(nwt) + b_n(z)\sin(nwt)\right), \quad (4)$$

where $w = 2\pi/365.25$ (day^{-1}). The first term is an altitude dependent constant. The second term L represents the linear time dependence. It can be a simple linear function

ACPD
13, 10661–10700, 2013
GOMOS-SAGE
E. Kyrölä et al.

of time, but we have selected it to be a piecewise linear function defined as

$$L(z,t) = \begin{cases} d_1(z)(t - t_c) & \text{if } t < t_c \\ d_2(z)(t - t_c) & \text{if } t \geq t_c. \end{cases} \quad (5)$$

It is parametrized by two slopes d_1, d_2 and the time of the inflexion point t_c. $F_{10.7}$, the solar 10.7 cm radio flux, is a proxy for solar influence on the middle atmosphere. F^{10}_{qbo} and F^{30}_{qbo} are the equatorial winds at 10 hPa and at 30 hPa, respectively, and are proxies for the Quasi-Biennial Oscillations (QBO). The observational basis for these proxies are discussed in Harris et al. (1999) and WMO (2007) and references therein. The last terms represent harmonic variation up to the second order, i.e. annual and semi-annual terms. The proxy terms are scaled in such a way that their time averages are zero, which makes it easier to compare their contributions with the harmonic and linear terms. The analysis is similar to the one in Kyrölä et al. (2010a).

The fitting is carried out as a classical least squares problem without data weighting. All latitudinal bands and altitudes are fitted separately without any regularization terms. The estimated uncertainties are modified by the residual correction term. In the fitting process we keep the inflexion time outside the parameter optimization. It is determined by looking for the best overall fit result when varying the inflexion year. The quality of the time series fit is analyzed by t values. Figure 11 shows how the t values change as a function of the inflexion year for high latitudes and for three altitudes. We can see that the inflexion time is clearly 1997–1998 for measurements near 40 km. For lower altitudes and lower latitudes the data do not support a clear turn around year. In our final analysis we accept the inflexion year 1997 for all fits. In Fig. 12 we show an example of the fit in the latitude band 40°–50° N at 30 km. While the fitted curve follows most of the data points, there are still several points falling out from the fit curve. One possible reason for these deviations is variation in temporal and/or latitudinal asymmetry as discussed in connection with the choice of the common grid. Unfortunately, it is impossible to explain these "outliers" in the time series using asymmetries without turning to

ACPD
13, 10661–10700, 2013

a priori data on ozone variability. This question will be addressed in the continuation paper (Laine et al., 2013).

As an example of the fitted proxy terms, we show in Fig. 13 the solar term as percentage to the constant term of Eq. (4). The solar term is scaled by the constant term of the time series fit. The statistically significant solar contribution is 1–3 % in the stratosphere and 2–4 % in the mesosphere. Note that the values are not totally symmetric around the Equator.

8 Ozone trend

The linear fitting coefficients in different latitude bands as a function of altitude are shown in Fig. 14 for 1984–1997 and in Fig. 15 for 1997–2011. Figure 16 shows the difference between the two trends.

The trend results for 1984–1997 in Fig. 14 show clear negative trends for all latitudes in the altitude range of 30–60 km. In the middle stratosphere the trend is −8 % per decade at high latitudes and −4 % in the tropics. In the lower stratosphere the trend values are less negative, but also the statistical uncertainty is large. In the mesosphere the trend varies between −2 % and −4 %. These results compare well with the results in Wang (2002). Figure 13 of this reference gives the ozone trend from 1984–1999 based on SAGE II measurements and data version 6.1. In addition to the difference in data version the statistical method used differs from the method of this work but overall the results show a reasonably good agreement.

The statistically significant trend results for 1997–2011 in Fig. 15 show that ozone at 38–45 km is now increasing at a rate of 2 % per decade. In the altitude range 30–35 km in the tropics we find an interesting region where ozone is still decreasing at a rate of −2–3 % per decade (first discussed in Gebhardt et al., unpublished, ACP, 2013). The latitudes outside 20° S–20° N in the lower stratosphere, 20–25 km, show large ozone depletion rates of 2 to 6 % per decade. In the mesosphere the decrease of ozone is still ongoing at a rate of 2–6 % per decade.

ACPD
13, 10661–10700, 2013

In Fig. 16 we show how the trends in the period 1997–2011 have changed compared to the ones in the period of 1984–1997. We find large statistically significant changes in trends at all latitudes in the 25–50 km altitude region. Largest changes, 6–10 % per decade, have occurred at high latitudes. In the lower stratosphere in the tropics the rates are by 2–5 % larger than in the period of 1984–1997 in the altitude range 20–25 km. Outside the tropics the decay trends have increased by 2–5 %. The peculiar 30–35 km region in the tropics shows also enhanced decay rates. The rate changes in the mesosphere vary from negative to positive.

9 Conclusions

We have created a homogenized ozone profile data set from SAGE II and GOMOS measurements for the period of 1984–2011. A significant bias between SAGE II sunrise and sunset data with respect to GOMOS nighttime measurements has been identified. The most plausible reason for the bias is diurnal variation of ozone in the stratosphere. In combining individual instrument data we have renormalized the SAGE II sunrise and sunset profiles so that they are not biased with respect to GOMOS measurements in the common operational period 2002–2005. The combined data set time series was then analyzed for trends in the stratosphere and mesosphere.

The combined SAGE II-GOMOS data set time series was analyzed using a linear regression model. This model includes a constant term, annual and semi-annual terms, solar and QBO proxies and a linear term with two independent slopes joining at the inflexion time. We found that year 1997 is the best estimate for the inflexion year of linear trends. The trend results for 1984–1997 show clear negative trends for all latitudes in the altitude range of 30–60 km. The trends for 1997–2010 are, however, close to zero or slightly positive except in the mesosphere, in lower stratosphere outside the tropics and in the isolated tropical island between 30–35 km. It is thought that the estimated trends are real trends of the ozone distribution and not artifacts from instrumental rifts.

ACPD
13, 10661–10700, 2013
GOMOS-SAGE
E. Kyrölä et al.

Acknowledgements. We would like to thank the Academy of Finland MIDAT project for financial support for this work. M. Laine has been supported by the Academy of Finland project number 132808. We want to thank T. Sakazaki and the SMILES team for sharing their work before publication.

References

Bertaux, J. L., Kyrölä, E., Fussen, D., Hauchecorne, A., Dalaudier, F., Sofieva, V., Tamminen, J., Vanhellemont, F., Fanton d'Andon, O., Barrot, G., Mangin, A., Blanot, L., Lebrun, J. C., Pérot, K., Fehr, T., Saavedra, L., Leppelmeier, G. W., and Fraisse, R.: Global ozone monitoring by occultation of stars: an overview of GOMOS measurements on ENVISAT, Atmos. Chem. Phys., 10, 12091–12148, doi:10.5194/acp-10-12091-2010, 2010. 10664, 10665

Bogumil, K., Orphal, J., Homann, T., Voigt, S., Spietz, P., Fleischmann, O., Vogel, A., Hartmann, M., Kromminga, H., Bovensmann, H., Frerick, J., and Burrows, J.: Measurements of molecular absorption spectra with the SCIAMACHY pre-flight model: instrument characterization and reference data for atmospheric remote-sensing in the 230–2380 nm region, J. Photochem. Photobiol. A, 157, 167–184, doi:10.1016/S1010-6030(03)00062-5, 2003. 10665, 10667

Burton, S. P., Thomason, L. W., and Zawodny, J. M.: Technical Note: Time-dependent limb-darkening calibration for solar occultation instruments, Atmos. Chem. Phys., 10, 1–8, doi:10.5194/acp-10-1-2010, 2010. 10665

Chu, W. P., McCormick, M. P., Lenoble, J., Brogniez, C., and Pruvost, P.: SAGE II inversion algorithm, J. Geophys. Res., 94, 8339–8351, 1989. 10664, 10665

Cunnold, D., Wang, H., Thomason, L., Zawodny, J., Logan, J., and Megretskaia, I.: SAGE (version 5.96) ozone trends in the lower stratosphere, J. Geophys. Res.-Atmos., 105, 4445–4457, 2000. 10665

Cunnold, D. M., Chu, W. P., McCormick, M. P., Veiga, R. E., and Barnes, R. A.: Validation of SAGE II ozone measurements, J. Geophys. Res., 94, 8447–8460, doi:10.1029/JD094iD06p08447, 1989. 10665

ESA: Envisat-GOMOS, An instrument for global atmospheric ozone monitoring, vol. SP-1244, European Space Agency, Noordwijk, The Netherlands, 2001. 10665

Harris, N., Hudson, R., and Phillips, C.: Assessment of trends in the vertical distribution of ozone, WMO, Geneva, 1999. 10663, 10675

Jones, A., Urban, J., Murtagh, D. P., Eriksson, P., Brohede, S., Haley, C., Degenstein, D., Bourassa, A., von Savigny, C., Sonkaew, T., Rozanov, A., Bovensmann, H., and Burrows, J.: Evolution of stratospheric ozone and water vapour time series studied with satellite measurements, Atmos. Chem. Phys., 9, 6055–6075, doi:10.5194/acp-9-6055-2009, 2009. 10663

Kyrölä, E., Tamminen, J., Sofieva, V., Bertaux, J. L., Hauchecorne, A., Dalaudier, F., Fussen, D., Vanhellemont, F., Fanton d'Andon, O., Barrot, G., Guirlet, M., Fehr, T., and Saavedra de Miguel, L.: GOMOS O_3, NO_2, and NO_3 observations in 2002–2008, Atmos. Chem. Phys., 10, 7723–7738, doi:10.5194/acp-10-7723-2010, 2010a. 10673, 10675

Kyrölä, E., Tamminen, J., Sofieva, V., Bertaux, J. L., Hauchecorne, A., Dalaudier, F., Fussen, D., Vanhellemont, F., Fanton d'Andon, O., Barrot, G., Guirlet, M., Mangin, A., Blanot, L., Fehr, T., Saavedra de Miguel, L., and Fraisse, R.: Retrieval of atmospheric parameters from GOMOS data, Atmos. Chem. Phys., 10, 11881–11903, doi:10.5194/acp-10-11881-2010, 2010b. 10666

McCormick, M., Zawodny, J., Veiga, R., Larsen, J., and Wang, P.: An overview of SAGE I and II ozone measurements, Planet. Space Sci., 37, 1567–1586, 1989. 10664

McPeters, R. D., Miles, T., Flynn, L. E., Wellemeyer, C. G., and Zawodny, J. M.: Comparison of SBUV and SAGE II ozone profiles: Implications for ozone trends, J. Geophys. Res., 99, 20513–20524, doi:10.1029/94JD02008, 1994. 10665

Meijer, Y. J., Swart, D. P. J., Allaart, M., Andersen, S. B., Bodeker, G., Boyd, I., Braathen, G., Calisesi, Y., Claude, H., Dorokhov, V., von der Gathen, P., Gil, M., Godin-Beekmann, S., Goutail, F., Hansen, G., Karpetchko, A., Keckhut, P., Kelder, H. M., Koelemeijer, R., Kois, B., Koopman, R. M., Kopp, G., Lambert, J.-C., Leblanc, T., McDermid, I. S., Pal, S., Schets, H., Stubi, R., Suortti, T., Visconti, G., and Yela, M.: Pole-to-pole validation of Envisat GOMOS ozone profiles using data from ground-based and balloon sonde measurements, Journal of Geophysical Research (Atmospheres), 109, D23305, doi:10.1029/2004JD004834, 2004. 10666

Nair, P. J., Godin-Beekmann, S., Pazmiño, A., Hauchecorne, A., Ancellet, G., Petropavlovskikh, I., Flynn, L. E., and Froidevaux, L.: Coherence of long-term stratospheric ozone vertical distribution time series used for the study of ozone recovery at a northern mid-latitude station, Atmos. Chem. Phys., 11, 4957–4975, doi:10.5194/acp-11-4957-2011, 2011. 10667

Nair, P. J., Godin-Beekmann, S., Froidevaux, L., Flynn, L. E., Zawodny, J. M., Russell III, J. M., Pazmiño, A., Ancellet, G., Steinbrecht, W., Claude, H., Leblanc, T., McDermid, S., van Gijsel, J. A. E., Johnson, B., Thomas, A., Hubert, D., Lambert, J.-C., Nakane, H., and Swart, D. P. J.: Relative drifts and stability of satellite and ground-based stratospheric ozone profiles at NDACC lidar stations, Atmos. Meas. Tech., 5, 1301–1318, doi:10.5194/amt-5-1301-2012, 2012. 10667

Newchurch, M. J., Yang, E.-S., Cunnold, D. M., Reinsel, G. C., Zawodny, J. M., and Russell, J. M.: Evidence for slowdown in stratospheric ozone loss: first stage of ozone recovery, J. Geophys. Res.-Atmos., 108, 4507, doi:10.1029/2003JD003471, 2003. 10663

Randel, W. J. and Wu, F.: A stratospheric ozone profile data set for 1979–2005: variability, trends, and comparisons with column ozone data, J. Geophys. Res.-Atmos., 112, D06313, doi:10.1029/2006JD007339, 2007. 10663

Sofieva, V. F., Tamminen, J., Haario, H., Kyrölä, E., and Lehtinen, M.: Ozone profile smoothness as a priori information in the inversion of limb measurements, Ann. Geophys., 22, 3411–3420, 2004, http://www.ann-geophys.net/22/3411/2004/. 10667

Sofieva, V. F., Vira, J., Kyrölä, E., Tamminen, J., Kan, V., Dalaudier, F., Hauchecorne, A., Bertaux, J.-L., Fussen, D., Vanhellemont, F., Barrot, G., and Fanton d'Andon, O.: Retrievals from GOMOS stellar occultation measurements using characterization of modeling errors, Atmos. Meas. Tech., 3, 1019–1027, doi:10.5194/amt-3-1019-2010, 2010. 10667

Solomon, S.: Stratospheric ozone depletion: a review of concepts and history, Rev. Geophys., 37, 275–316, 1999. 10663

Staehelin, J., Harris, N. R. P., and Appenzeller, C.: Ozone trends: a review, Rev. Geophys., 39, 231–290, 2001. 10663

Steele, H. M. and Turco, R. P.: Separation of aerosol and gas components in the Halogen Occultation Experiment and the Stratospheric Aerosol and Gas Experiment (SAGE) II extinction measurements: implications for SAGE II ozone concentrations and trends, J. Geophys. Res., 1021, 19665–19682, doi:10.1029/97JD01263, 1997. 10665

Steinbrecht, W., Claude, H., Schönenborn, F., McDermid, I. S., Leblanc, T., Godin, S., Song, T., Swart, D. P. J., Meijer, Y. J., Bodeker, G. E., Connor, B. J., Kämpfer, N., Hocke, K., Calisesi, Y., Schneider, N., de la Noë, J., Parrish, A. D., Boyd, I. S., Brühl, C., Steil, B., Giorgetta, M. A., Manzini, E., Thomason, L. W., Zawodny, J. M., McCormick, M. P., Russell, J. M., Bhartia, P. K., Stolarski, R. S., and Hollandsworth-Frith, S. M.: Long-term evolution of upper stratospheric ozone at selected stations of the Network for the Detection of Stratospheric Change (NDSC), J. Geophys. Res.-Atmos., 111, D10308, doi:10.1029/2005JD006454, 2006. 10663

Steinbrecht, W., Claude, H., Schonenborn, F., McDermid, I. S., Leblanc, T., Godin-Beekmann, S., Keckhut, P., Hauchecorne, A., van Gijsel, J. A. E., Swart, D. P. J., Bodeker, G. E., Parrish, A., Boyd, I. S., Kampfer, N., Hocke, K., Stolarski, R. S., Frith, S. M., Thomason, L. W., Remsberg, E. E., von Savigny, C., Rozanov, A., and Burrows, J. P.: Ozone and temperature trends in the upper stratosphere at five stations of the Network for the Detection of Atmospheric Composition Change, Int. J. Remote Sens., 30, 3875–3886, doi:10.1080/01431160902821841, 2009. 10663

Tamminen, J., Kyrölä, E., Sofieva, V. F., Laine, M., Bertaux, J.-L., Hauchecorne, A., Dalaudier, F., Fussen, D., Vanhellemont, F., Fanton-d'Andon, O., Barrot, G., Mangin, A., Guirlet, M., Blanot, L., Fehr, T., Saavedra de Miguel, L., and Fraisse, R.: GOMOS data characterisation and error estimation, Atmos. Chem. Phys., 10, 9505–9519, doi:10.5194/acp-10-9505-2010, 2010. 10666

van Gijsel, J. A. E., Swart, D. P. J., Baray, J.-L., Bencherif, H., Claude, H., Fehr, T., Godin-Beekmann, S., Hansen, G. H., Keckhut, P., Leblanc, T., McDermid, I. S., Meijer, Y. J., Nakane, H., Quel, E. J., Stebel, K., Steinbrecht, W., Strawbridge, K. B., Tatarov, B. I., and Wolfram, E. A.: GOMOS ozone profile validation using ground-based and balloon sonde measurements, Atmos. Chem. Phys., 10, 10473–10488, doi:10.5194/acp-10-10473-2010, 2010. 10666

Wang, H., Cunnold, D., and Bao, X.: A critical analysis of stratospheric aerosol and gas experiment ozone trends, J. Geophys. Res., 101, 12495–12514, 1996. 10665

Wang, H. J.: Assessment of SAGE version 6.1 ozone data quality, Journal of Geophysical Research, 107, 1–18, doi:10.1029/2002JD002418, http://www.agu.org/pubs/crossref/2002/2002JD002418.shtml, 2002. 10665, 10676

Wang, P.-H., McCormick, M. P., Chu, W. P., Lenoble, J., Nagatani, R. M., Chanin, M. L., Barnes, R. A., Schmidlin, F., and Rowland, M.: SAGE II stratospheric density and temperature retrieval experiment, Journal of Geophysical Research, 97, 843–863, doi:10.1029/91JD02601, 1992. 10665

Weatherhead, E. C., Reinsel, G. C., Tiao, G. C., Jackman, C. H., Bishop, L., Hollandsworth Firth, S. M., Deluisi, J., Keller, T., Oltmans, S. J., Fleming, E. L., Wuebbles, D. J., Kerr, J. B., Miller, A. J., Herman, J., and McPeters, R.: Detecting the recovery of total column ozone, J. Geophys. Res., 105, 22201–22210, 2000. 10663

WMO: Scientific Assessment of Ozone Depletion: 2006, Global Ozone Research and Monitoring Project – Report No. 50, World Meteorological Organization, Geneva, Switzerland, 2007. 10675

WMO: Scientific Assessment of Ozone Depletion: 2010, Global Ozone Research and Monitoring Project – Report No. 52, World Meteorological Organization, Geneva, Switzerland, 2011. 10663

ACPD

13, 10661–10700, 2013

GOMOS-SAGE

E. Kyrölä et al.

Table 1. SAGE II and GOMOS (UV-Vis) retrieval compared.

Element	GOMOS IPF 6	SAGE II v. 7
Refraction	ray bending, dilution, scintillations	ray bending
Forward model	absorption by O_3, NO_2, NO_3; scattering ext. by air and aerosols	absorption by O_3, NO_2; scattering ext. by air and aerosols
Wavelengths	250–680 nm, 1416 pixels	386, 448, 453, 525, 600, 940 and 1020 nm
Rayleigh extinction	Removed using ECMWF	Removed using MERRA
Species separation	Simultaneously	Channel by channel
Vertical inversion	Onion peel with target resolution Tikhonov and the constraint of density continuity.	Onion peeling without smoothing
Ozone cross section	Bogumil et al.	Bogumil et al.
Local time	10 p.m.	Sunrise and sunset
Vertical sampling	0.2–1.7 km	Scanning
Vertical resolution	2 km (up to 30 km); 3 km above 40 km	1 km

ACPD
13, 10661–10700, 2013

Table 2. SAGE II and GOMOS filling factors for various grids (%).

Time × Latitude grid	SAGE II	GOMOS
1 d × 5 deg	7	20
1 d × 10 deg	12	34
1 d × 20 deg	21	51
3 d × 5 deg	14	26
3 d × 10 deg	18	40
3 d × 5 deg	27	50
5 d × 5 deg	20	30
5 d × 10 deg	24	44
5 d × 20 deg	33	59
1 Month × 5 deg	73	61
1 Month × 10 deg	76	71
1 Month × 20 deg	83	82

ACPD
13, 10661–10700, 2013

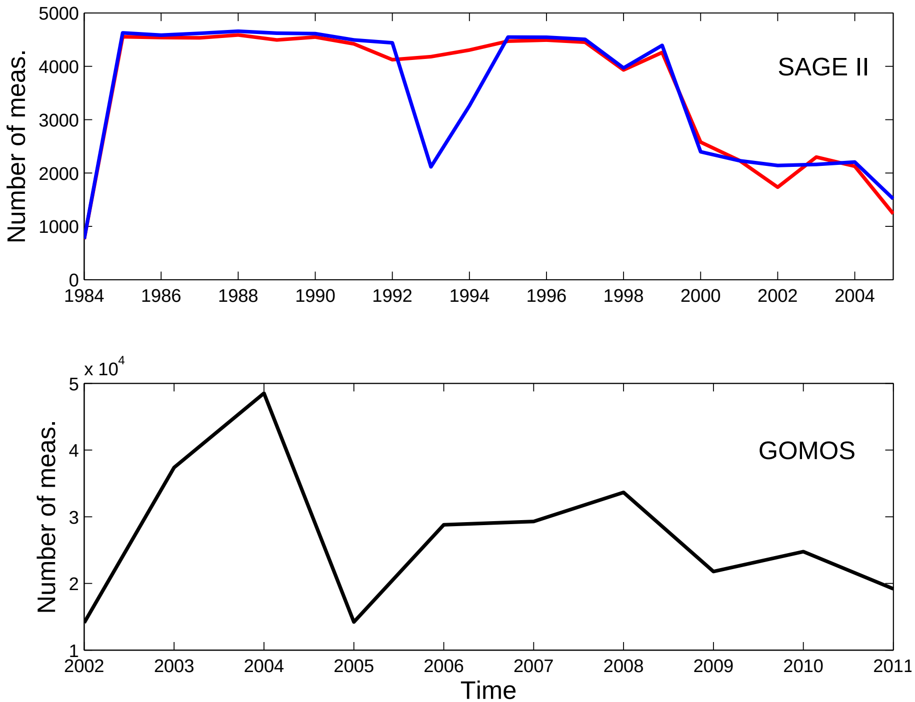

Fig. 1. The number of SAGE II sunrise (red)/sunset (blue) measurements for 1984–2005 and GOMOS measurements (black) for 2002–2011.

ACPD
13, 10661–10700, 2013

GOMOS-SAGE

E. Kyrölä et al.

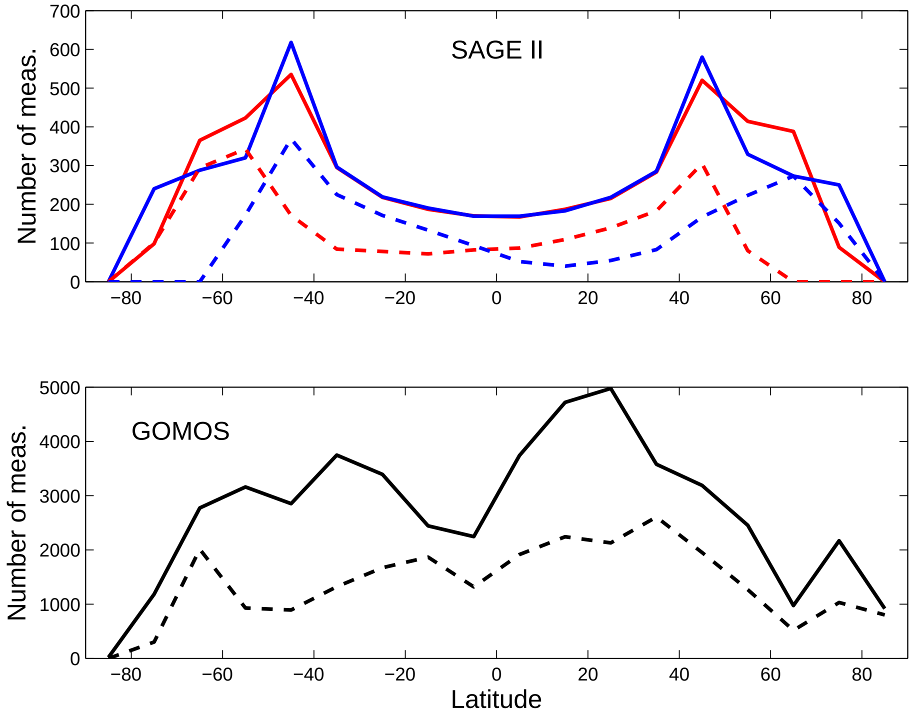

Fig. 2. Latitude distributions of SAGE II (top) and GOMOS (bottom) measurements. Notation: Solid and dashed red: SAGE II sunrise in 1985 and 2004, solid and dashed blue: SAGE II sunset in 1985 and 2004, solid and dashed black: GOMOS in 2004 and 2010.

ACPD
13, 10661–10700, 2013

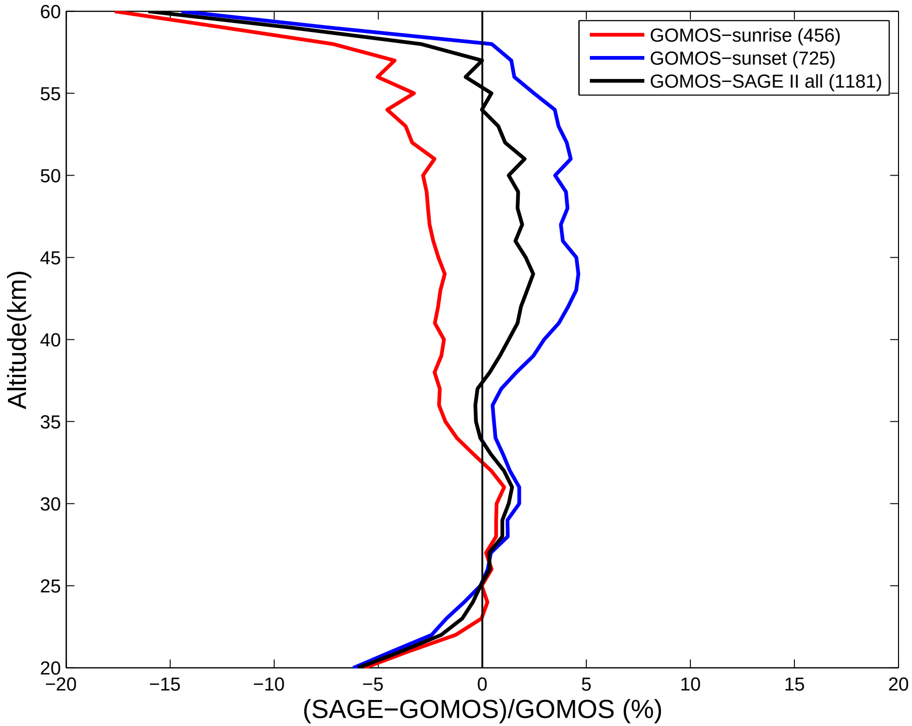

Fig. 3. The percent difference between SAGE II and GOMOS measurements for the collocations in 2002–2005. The corresponding differences betweenf SAGE II sunrise and sunset measurements are also shown.

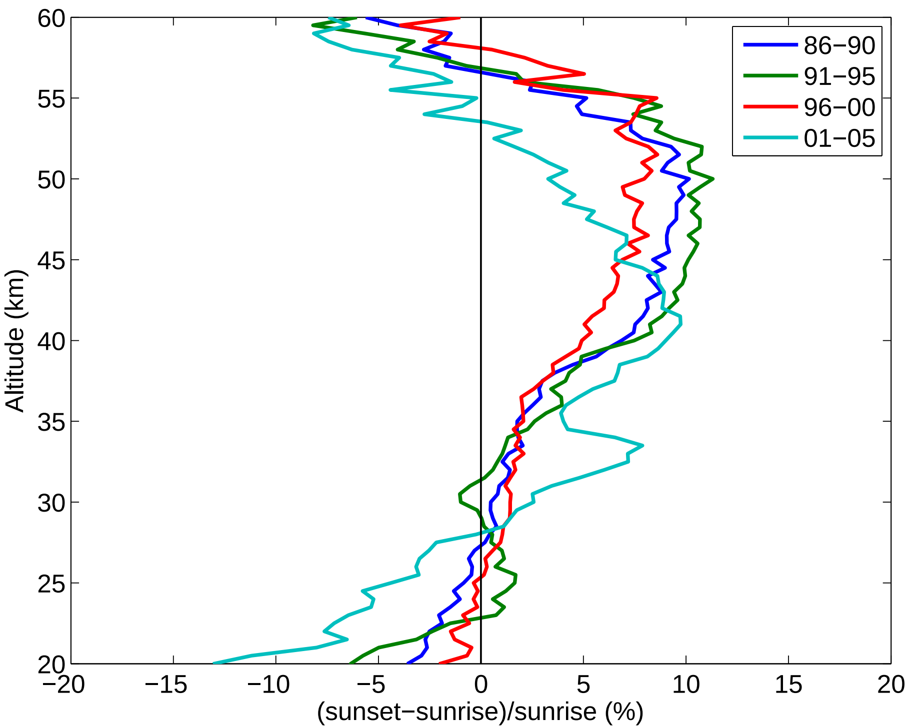

Fig. 4. SAGE II ozone sunrise measurements compared to sunset measurements for 5 yr periods in the tropics 10° S–10° N.

ACPD
13, 10661–10700, 2013

GOMOS-SAGE

E. Kyrölä et al.

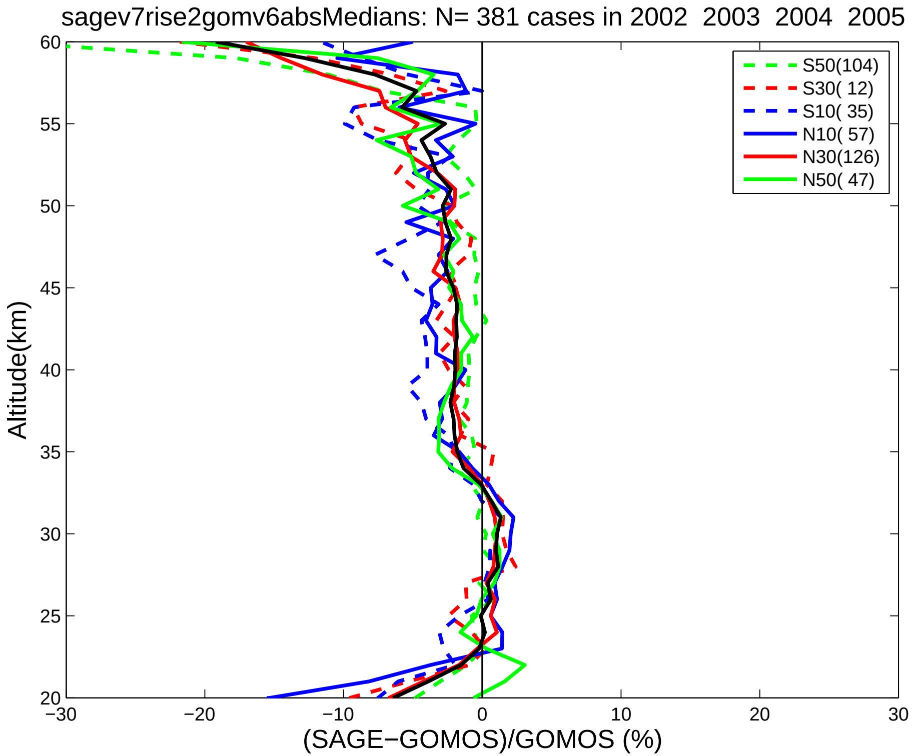

Fig. 5. The percent differences between SAGE II sunrise to GOMOS nighttime measurements in 20° latitude bands.

ACPD
13, 10661–10700, 2013

GOMOS-SAGE

E. Kyrölä et al.

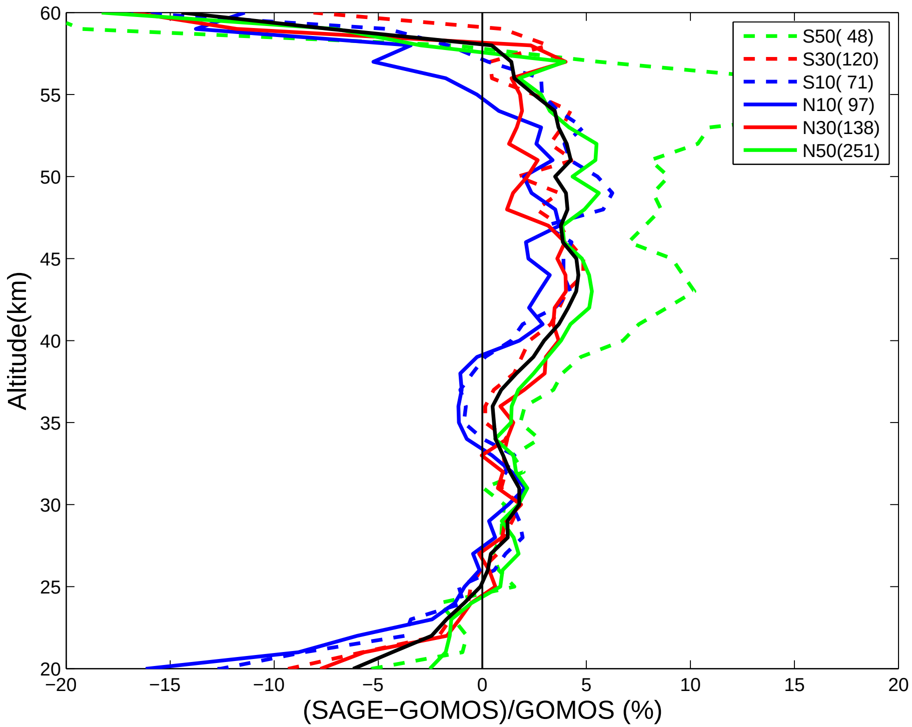

Fig. 6. The percent differences of SAGE II sunset to GOMOS nighttime measurements in 20° latitude bands.

ACPD
13, 10661–10700, 2013

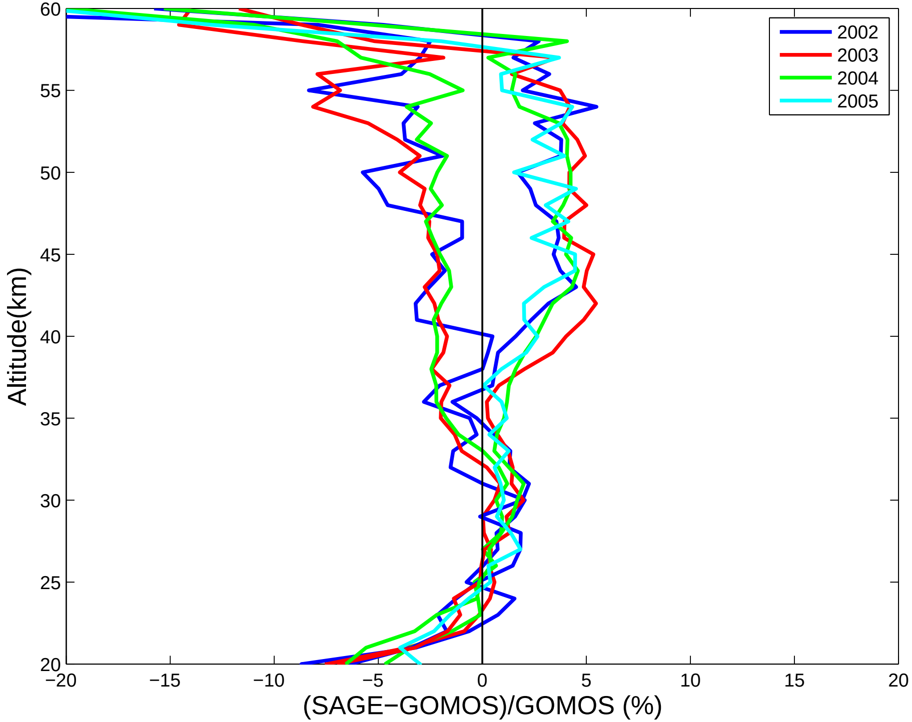

Fig. 7. The percent differences between SAGE II sunrise (mainly in left part of the figure) and sunset (mainly in right part of the figure) measurements and GOMOS nighttime ozone measurements as a function of measurement year.

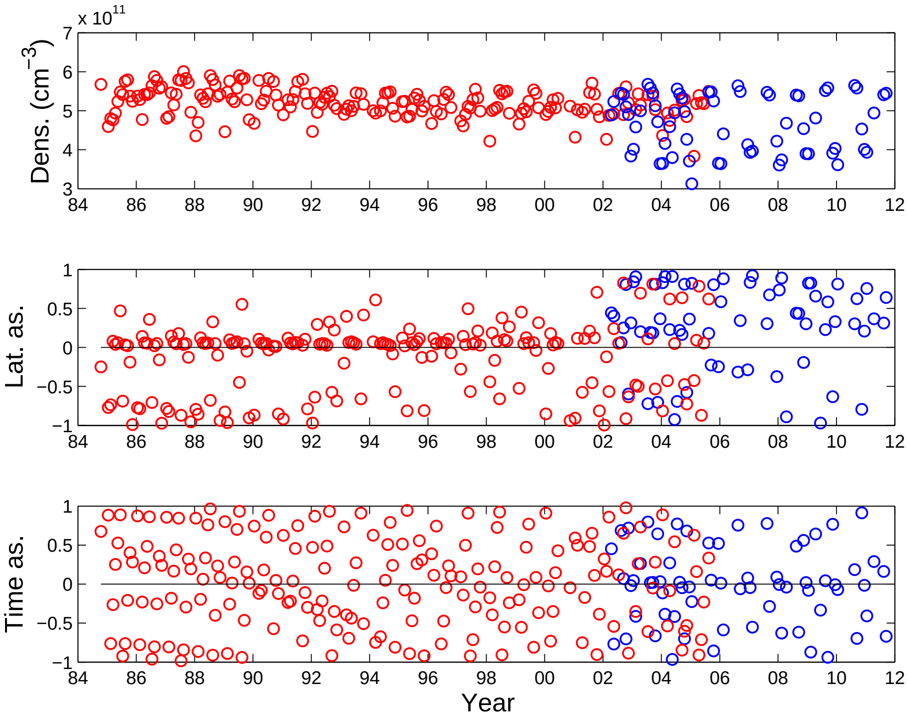

Fig. 8. Asymmetries in the 50°–60° N latitude range. Top: densities at 40 km, middle: latitude asymmetries, bottom: time asymmetries. Red circles are for SAGE II and blue circles for GOMOS data.

ACPD
13, 10661–10700, 2013

GOMOS-SAGE

E. Kyrölä et al.

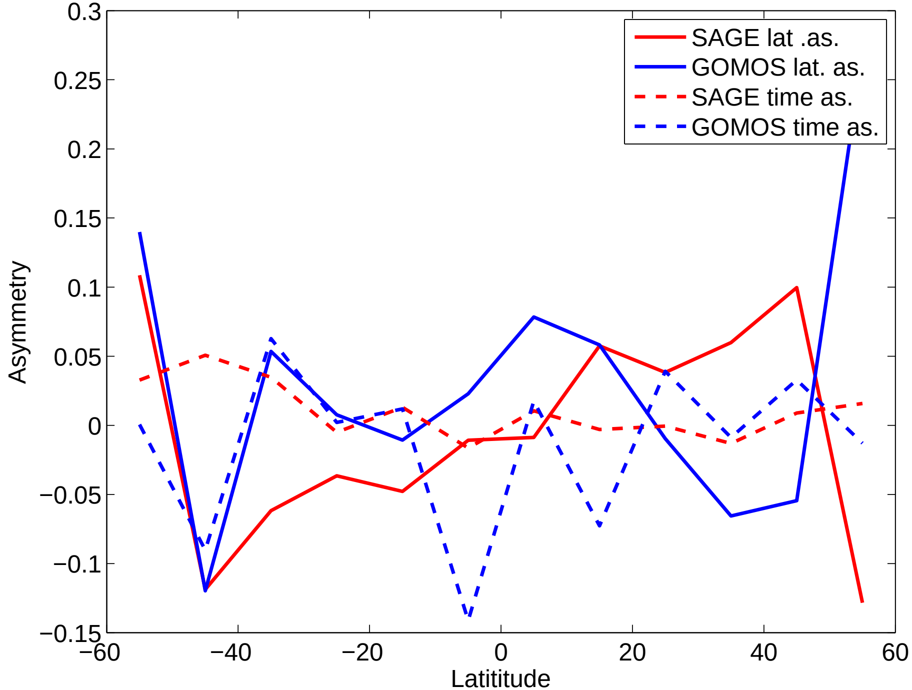

Fig. 9. The mean latitudinal and temporal asymmetries as a function of latitude.

ACPD
13, 10661–10700, 2013

GOMOS-SAGE

E. Kyrölä et al.

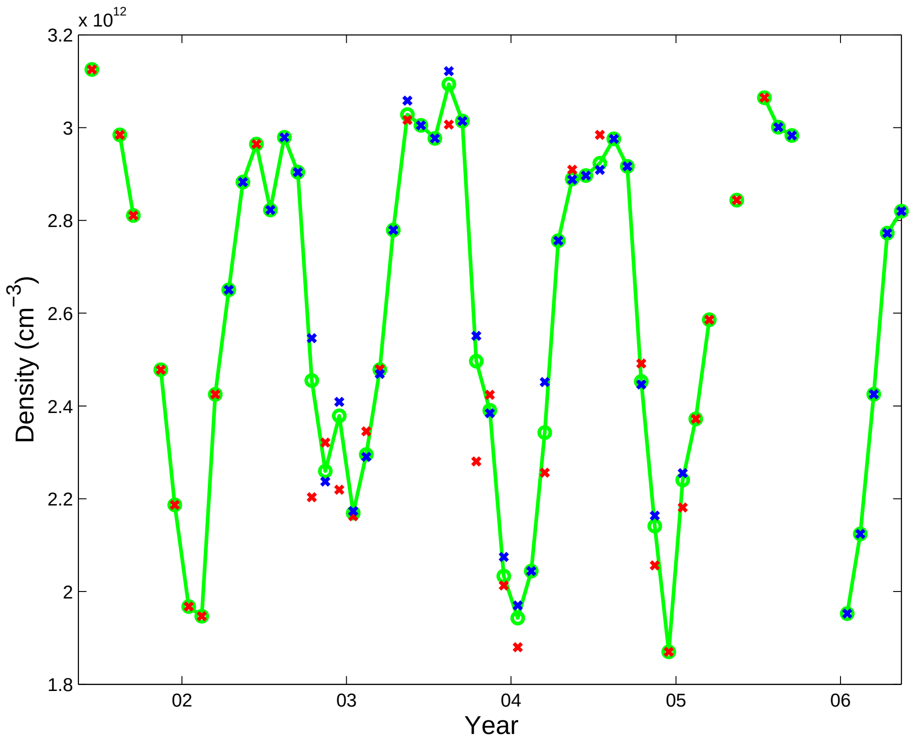

Fig. 10. An example of the combined SAGE II and GOMOS data sets at 30 km between 40° N–50° N. Red crosses indicate SAGE II data, blues crosses indicate GOMOS data, and the green line with circles indicates the combined data.

ACPD
13, 10661–10700, 2013

GOMOS-SAGE

E. Kyrölä et al.

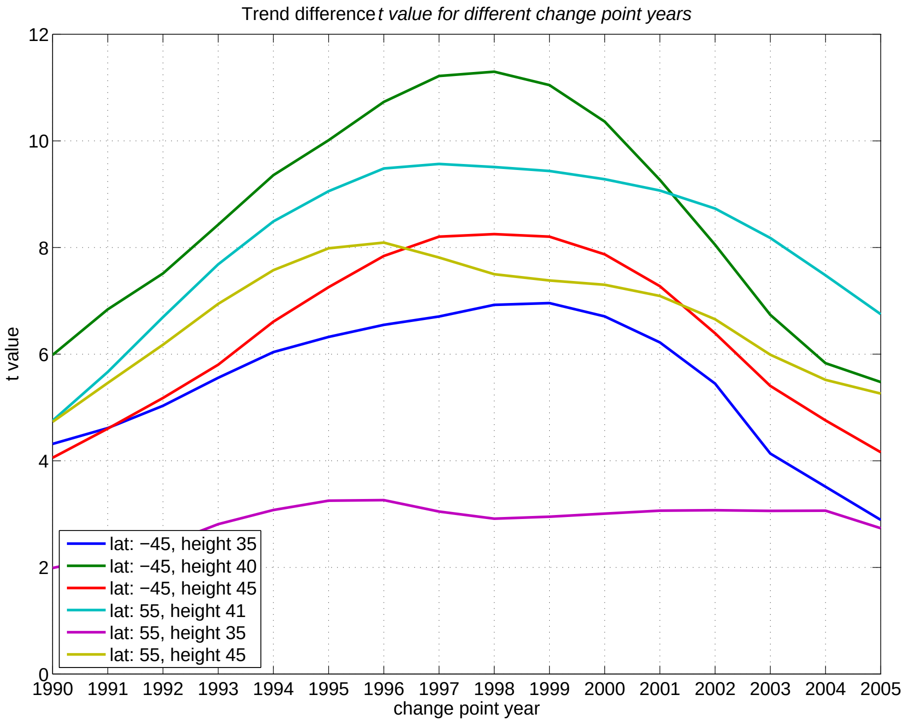

Fig. 11. The t values for the difference of trend terms at different latitudes and altitudes as a function of the inflexion year.

ACPD
13, 10661–10700, 2013

GOMOS-SAGE

E. Kyrölä et al.

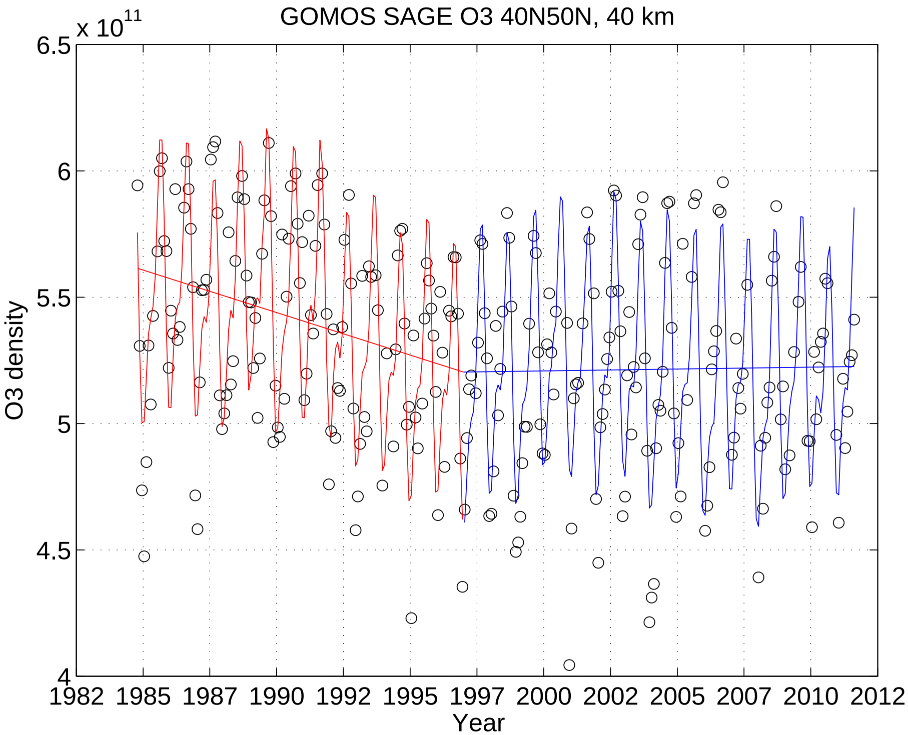

Fig. 12. An example of the fit at 40 km between 40°–50° N for the combined SAGE II-GOMOS data. The data points are black circles. The inflexion year is 1997. The red solid curve and red line line represent the fit and linear trend for 1984–1997, respectively. The blue solid curve and blue line represent the fit and linear trend for 1997–2011, respectively.

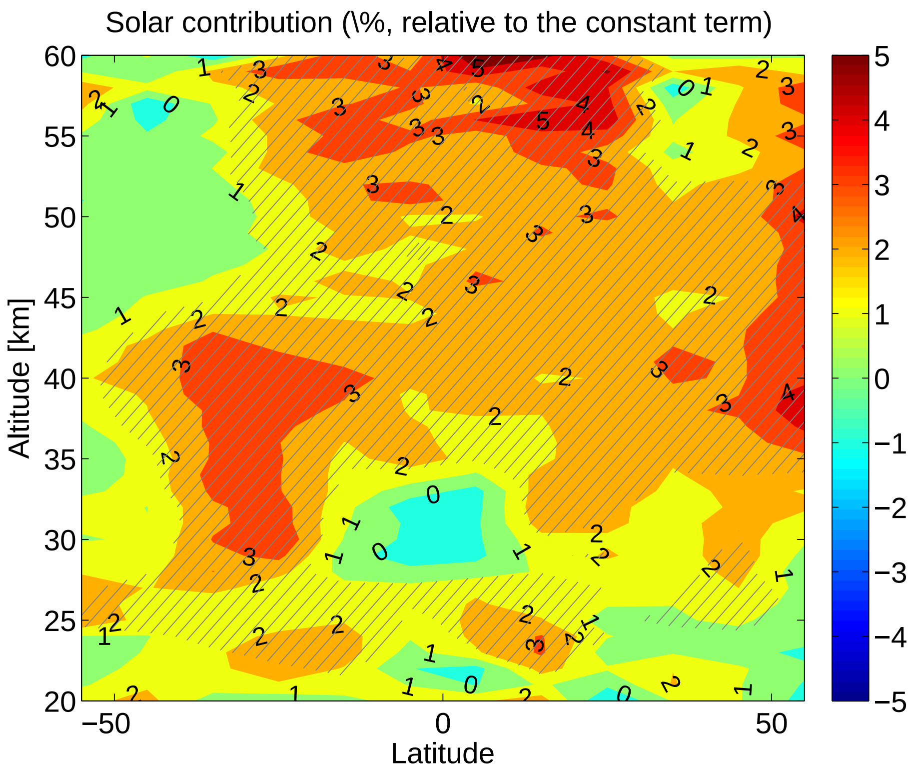

Fig. 13. The relative contribution of the solar proxy (%) with respect to the constant term. Shaded areas show regions where trends are statistically different from zero at the 95 % level.

ACPD
13, 10661–10700, 2013

GOMOS-SAGE

E. Kyrölä et al.

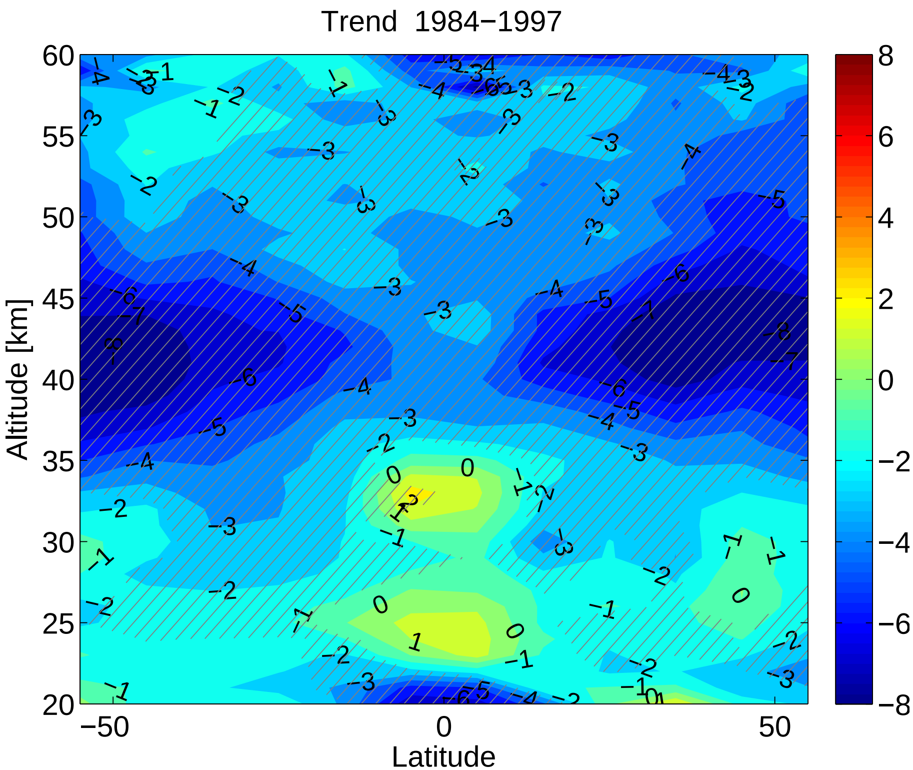

Fig. 14. The ozone trend in % per decade for different latitudes for1984–1997. Shaded areas show regions where trends are statistically different from zero at the 95 % level.

ACPD
13, 10661–10700, 2013

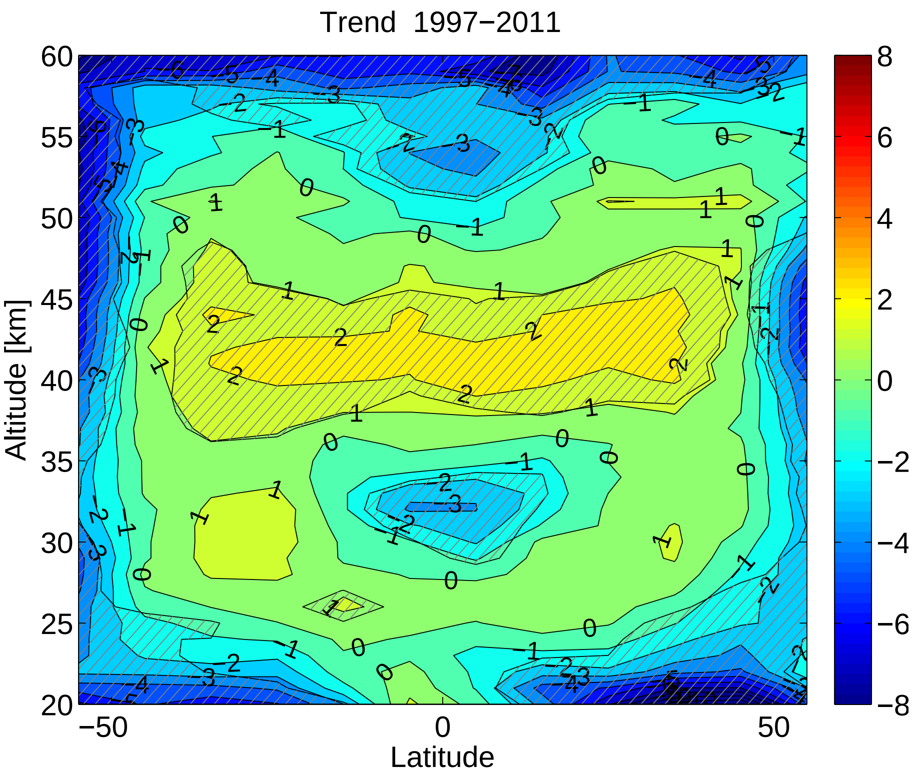

Fig. 15. The ozone trend in % per decade for different latitudes for 1997–2011. Shaded areas show regions where trends are statistically different from zero at the 95 % level.

ACPD
13, 10661–10700, 2013

GOMOS-SAGE

E. Kyrölä et al.

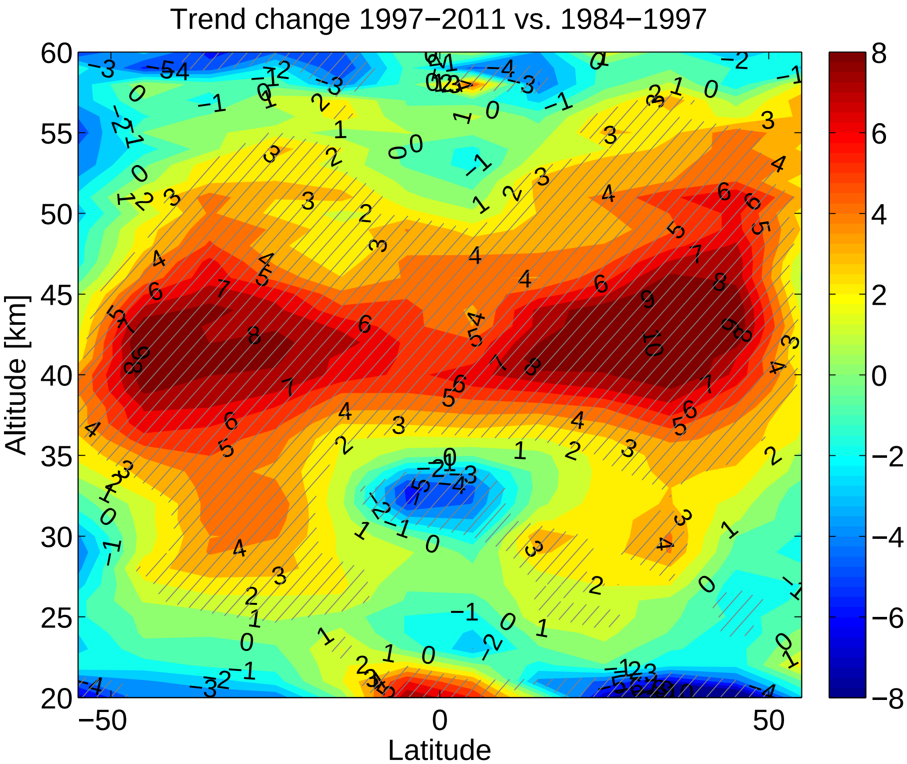

Fig. 16. The change in ozone trends in % per decade between the periods 1997–2011 and 1984–1997 at different latitudes. Shaded areas show regions where trend differences are statistically different from zero at the 95 % level.

ACPD
13, 10661–10700, 2013

GOMOS-SAGE

E. Kyrölä et al.